

**OPEN ACCESS**

## Unscreened cross-sections for nuclear astrophysics via the Trojan Horse Method

To cite this article: A Tumino *et al* 2014 *J. Phys.: Conf. Ser.* **569** 012018

View the [article online](#) for updates and enhancements.

### You may also like

- [BIG BANG NUCLEOSYNTHESIS REVISITED VIA TROJAN HORSE METHOD MEASUREMENTS](#)  
R. G. Pizzone, R. Spartá, C. A. Bertulani et al.
- [New measurement of the  \$^{10}\text{B}\(n,\gamma\)^7\text{Li}\$  through the Trojan Horse Method](#)  
Roberta Spartá
- [Effectiveness of using a magnetic spectrograph with the Trojan Horse method](#)  
S. Manwell, A. Parikh, A. A. Chen et al.



The Electrochemical Society  
Advancing solid state & electrochemical science & technology

243rd Meeting with SOFC-XVIII

Boston, MA • May 28 – June 2, 2023

**Accelerate scientific discovery!**

Learn More & Register



# Unscreened cross-sections for nuclear astrophysics via the Trojan Horse Method

**A. Tumino<sup>1,2</sup>, C. Spitaleri<sup>1,3</sup>, M. La Cognata<sup>1,3</sup>, L. Lamia<sup>1,3</sup>,  
R.G. Pizzone<sup>1,3</sup>, M.L. Sergi<sup>1,3</sup>**

<sup>1</sup>Laboratori Nazionali del Sud - INFN, Catania, Italy

<sup>2</sup>Università degli Studi di Enna “Kore”, Enna, Italy

<sup>3</sup>Dipartimento di Metodologie Fisiche e Chimiche per l’Ingegneria - Università di Catania, Catania, Italy

E-mail: tumino@lns.infn.it

**Abstract.** The bare nucleus astrophysical  $S(E)$  factor is the Nuclear Physics parameter to determine the reaction rates in stellar plasmas. Whilst not being accessed in direct measurements, it can be easily determined using the Trojan Horse Method, successful indirect technique for nuclear astrophysics. The basic features of the method will be discussed and some recent results will be presented.

## 1. Introduction

The cross sections of nuclear reactions relevant for astrophysics are key parameters to better understand the stellar evolution. For this reason they should be measured at the Gamow energy. There are many different types of stars and each has its own unique set of nuclear reactions that change in character as the star evolves, in particular towards the end of its life. In spite of the great efforts to measure the rates of the most relevant reactions, there is still considerable uncertainty about their values. This is due to the difficulty to measure the rates at the Gamow energy. Although temperatures involved are high, on the order of hundred million degrees, the corresponding reaction rates are extremely small, making it difficult for them to be measured directly in the laboratory. Indeed, for charged particle reactions the Coulomb barrier causes a strong suppression of the cross-section, which drops exponentially with decreasing energy. The standard way to determine the behavior of  $\sigma(E)$  at low energy is the extrapolation from higher energies (usually  $E > 100$  keV) by means of the astrophysical  $S(E)$ -factor

$$S(E) = E\sigma(E) \exp(2\pi\eta), \quad (1)$$

with  $\eta$  the Coulomb parameter of the colliding nuclei, and  $\exp(2\pi\eta)$  the inverse of the Gamow factor that removes the energy dependence of  $\sigma(E)$  due to the barrier tunneling. However, even an easier extrapolation can be source of additional uncertainties for  $\sigma(E)$  due, for instance, to the presence of unexpected resonances.

Another critical issue in the laboratory measurement of nucleosynthesis processes is represented by the electron screening effect. Indeed both target and projectile are usually embedded in neutral/ionized atoms or molecules and their electron clouds are responsible for a



reduction of the Coulomb barrier. This, in turn, leads to an increased cross section for screened nuclei,  $\sigma_s(E)$ , compared to the cross section for bare nuclei  $\sigma_b(E)$  [1, 2]. Therefore, the so called screening factor, defined as

$$f_{\text{lab}}(E) = \sigma_s(E)/\sigma_b(E) \approx \exp(\pi\eta U_e/E), \quad (2)$$

where  $U_e$  is the so-called "electron screening potential" [1, 2], has to be taken into account to determine the bare nucleus cross section.

In the stellar plasma, the cross section  $\sigma_{pl}(E)$  is related to the bare nucleus cross section by a similar enhancement factor:

$$f_{pl}(E) = \sigma_{pl}(E)/\sigma_b(E) \approx \exp(\pi\eta U_{pl}/E) \quad (3)$$

that can be calculated once the plasma screening potential  $U_{pl}$  is known, depending on important properties of the plasma such as the Debye-Hückel radius. A measurement of  $U_e$ , which is needed to calculate  $\sigma_s(E)$  from Eq. 2, would also help to better understand  $U_{pl}$ .

Low-energy fusion reactions measured so far have indeed shown the exponential enhancement according to equation (2)[2]. However, the deduced  $U_e$  values are larger than the adiabatic limit, provided by the atomic models as the difference between the electron binding energies of the separate atoms in the entrance channel and that of the composite atom [2, 3]. This disagreement in laboratory experiments is yet to be justified, and prevents the effects under astrophysical conditions to be fully understood.

A weak point in the laboratory approach - and thus in the deduced  $U_e$  value - is the necessity to make an assumption for the energy dependence of  $\sigma_b(E)$  at ultra-low energies. Thus, indirect techniques ([4] and references therein) such as the Trojan Horse Method (THM) ([5] and references therein), have been introduced to overcome all these difficulties. In particular, the THM has been successfully applied to determine  $\sigma_b(E)$  for reactions between charged particles. Here we recall the basic ideas of the THM and we show some recent results.

## 2. Short Description of Trojan Horse Method

The THM ([5, 6, 7] and references therein) makes use of an appropriate  $A + a \rightarrow c + C + s$  two-to-three body process to measure the astrophysical  $A + x \rightarrow c + C$  two-body reaction of interest by establishing a relation between the two reactions based on the nuclear reaction theories. The three-body process is chosen in such a way that target  $a$  (or equivalently the projectile) is described in terms of the  $x \oplus s$  cluster structure with  $x$  the target (or equivalently the projectile) of the two-body reaction. The selected part of the three-body phase space is the one where the quasi free kinematics applies: the other cluster  $s$  remains spectator to the process, and  $A + x \rightarrow c + C$  can be regarded as an half-off-energy-shell (HOES) two-body reaction, usually referred to as a quasi-free reaction. Since the three-body process occurs at an energy above the Coulomb barrier, the main feature is the real suppression of both Coulomb barrier and screening effects in the HOES two-body cross section. Nevertheless, the quasi-free  $A + x$  process can occur even at very low sub-Coulomb energies because the  $A + a$  relative motion is compensated for by the  $x - s$  binding energy. This is indeed a different approach to the THM [5] compared to the original idea of Baur [8], where the initial velocity of the projectile  $A$  is compensated for by the  $x - s$  intercluster motion. In that framework a quite large momentum of the order of 200 MeV/c or more is needed. But the relative yield of the experimental momentum distribution at such momenta can be very small, in particular for a  $l=0$  inter-cluster motion (for example p-n motion inside  $^2\text{H}$  or  $\alpha$ -d motion inside  $^6\text{Li}$ ). This would make very critical the separation from other competitive reaction mechanisms. Moreover, the theoretical description of the tails of the momentum distribution is a hard task, their shape being very sensitive to it. In our approach to the THM, the intercluster motion is only needed to determine the accessible astrophysical

energy region. It corresponds to a cutoff in momentum distribution of  $s$  of few tens of MeV/c. In this framework, the so called ”quasi-free two-body energy” is given by:

$$E_{QF} = \frac{m_x}{m_x + m_A} E_A - B_{x-s}. \quad (4)$$

where  $E_A$  represents the beam energy,  $m_x$  and  $m_A$  are the masses of  $x$  and  $A$  particles respectively, and  $B_{x-s}$  is the binding energy for the  $x - s$  system.

In the Impulse Approximation, based essentially on the assumption that the interaction of the spectator with particles  $C$  and  $c$  is neglected, the three body-cross section can be factorized as:

$$\frac{d^3\sigma}{dE_c d\Omega_c d\Omega_C} \propto [KF |\varphi_a(\mathbf{p}_{sx})|^2] \left( \frac{d\sigma}{d\Omega_{c.m.}} \right)^{\text{HOES}} \quad (5)$$

where KF is a kinematical factor containing the final state phase-space factor. It is a function of the masses, momenta and angles of the outgoing particles [30];  $\varphi_a(\mathbf{p}_{sx})$  is proportional to the Fourier transform of the radial wave function  $\chi(\mathbf{r})$  for the  $x - s$  inter-cluster relative motion;  $(d\sigma/d\Omega_{c.m.})^{\text{HOES}}$  is the HOES differential cross section for the binary reaction at the center of mass energy  $E_{c.m.}$  given in post-collision prescription by

$$E_{c.m.} = E_{cC} - Q_{2b}. \quad (6)$$

Here,  $Q_{2b}$  is the  $Q$ -value of the binary reaction and  $E_{cC}$  is the relative energy of the outgoing particles  $c$  and  $C$ , which spans the accessible astrophysical region defined above.

The factorization of Eq.5 is strictly valid in Plane Wave Impulse Approximation, which changes only the absolute magnitude but not the energy dependence of the two-body cross section.

### 3. Experimental Details

In THM experiments, the decay products ( $c$  and  $C$ ) of the virtual two-body reaction of interest are usually detected and identified by means of telescopes (silicon detector or ionization chamber as  $\Delta E$  detector and PSD as  $E$  detector) placed in a phase space region where quasi free kinematics is dominant. After the selection of the reaction channel, a critical point is the separation of the quasi free mechanism from other reaction mechanisms feeding the same particles in the final state, e.g. sequential decay and direct break-up. An observable which is very sensitive to the reaction mechanism is the shape of the experimental momentum distribution  $\Phi(p_s)$  of the spectator. To reconstruct the experimental  $\Phi(p_s)$  distribution, the energy sharing method [9] can be applied for each pair of coincidence QF angles: the quasi-free coincidence yield with a cutoff in relative energy of few hundreds of keV at most is divided by the kinematic factor, providing a quantity which is proportional to the product of the momentum distribution for the spectator with the differential two-body cross section (see Eq.5). The window is chosen in such a way that the differential two-body cross section in this range can be considered almost constant. Thus, the quantity defined above represents essentially the momentum distribution for the spectator that in PWIA can be compared with the Fourier transform of the radial  $x - s$  bound state wave function.

Data analysis is limited to the region where the agreement between the two distributions exists. Usually a window of few tens of MeV/c is chosen not to move too far from  $E_{QF}$ , according to the prescriptions reported in [15]. Therefore,  $((d\sigma/d\Omega_{cm})^{\text{HOES}})$  can be extracted from the three-body coincidence yield by simply inverting Eq.5. The Coulomb barrier in  $((d\sigma/d\Omega_{cm})^{\text{HOES}})$  is suppressed [10] and this is due to the virtuality of particle  $x$ . This seems to be the only consequence of off-energy-shell effects as suggested by the agreement between HOES and on-energy-shell (OES) cross-sections for the  ${}^6\text{Li}(n,\alpha){}^3\text{H}$  reaction [11].

The suppression of the Coulomb barrier has been tested also in scattering processes addressing the study of the  $p+p$  elastic scattering through the  ${}^2\text{H}(p, pp)n$  reaction as reported in [12, 13]. All experimental works provided so far provide conclusive evidence of the suppression of Coulomb effects in the THM method.

Thus, in a final step, to relate the HOES excitation function to the relevant OES one, Coulomb corrections have to be considered. If one looks at the angular distributions no correction is needed because once the energy is fixed, it would mean to introduce simply a scaling factor. Thus, the OES data are directly comparable with HOES ones projected onto the emission angle of  $C$  (or  $c$ ) in the  $C - c$  center of mass system,  $\theta_{c.m.}$ , as given by [16]:

$$\theta_{c.m.} = \arccos \frac{(\mathbf{v}_A - \mathbf{v}_x) \cdot (\mathbf{v}_c - \mathbf{v}_C)}{|\mathbf{v}_A - \mathbf{v}_x| |\mathbf{v}_c - \mathbf{v}_C|} \quad (7)$$

where the vectors  $\mathbf{v}_A$ ,  $\mathbf{v}_x$ ,  $\mathbf{v}_c$ ,  $\mathbf{v}_C$  are the velocities of projectile, transferred particle and outgoing nuclei respectively. These quantities are calculated from their corresponding momenta in the lab-system, where the momentum of the transferred particle is equal and opposite to that of  $s$  when the quasi-free break-up takes place in the target, otherwise a little different formula has to be used [16]. If HOES data are projected onto the  $E_{Cc}$  axis, Coulomb suppression has to be introduced before comparison with OES data. In a simple approach this is done by means of the penetrability factor:

$$P_l(k_{Ax}R) = \frac{1}{G_l^2(k_{Ax}R) + F_l^2(k_{Ax}R)} \quad (8)$$

with  $F_l$  and  $G_l$  regular and irregular Coulomb wave functions and  $R$  the so called cutoff radius [22], which is usually chosen as the sum of the radii of nuclei  $A$  and  $x$ . This procedure does not provide the absolute value of the two-body cross section that can be easily derived from a scaling to the direct data available at higher energies.

#### 4. Applications

The THM has been applied already many times to charged particle reactions connected with fundamental astrophysical problems [17], from Big-Bang to stellar nucleosynthesis. A list of reactions studied by means of the THM is given in Table 1 together with the relevant references. In particular, low-energy cross sections for reactions producing or destroying Lithium isotopes are fundamental for several astrophysical problems yet to be solved, e.g. understanding Big Bang nucleosynthesis and the "Lithium depletion" in the Sun or in other galactic stars. In addition they offer very clear examples on the capabilities of the method in measuring the bare nucleus cross section. An experimental program was undertaken to study p-capture reactions on  ${}^6,{}^7\text{Li}$ , main responsible for their destruction [18, 19, 22, 23, 24, 25, 26, 27, 28, 29, 50]. The extracted astrophysical  $S(E)$  factors were compared with those from direct measurements and found in fair agreement in the energy range where screening effects are negligible. Recently, an updated reaction rate for the  ${}^6\text{Li}(p, \alpha){}^3\text{He}$  reaction has been determined using direct data of [53, 54] for a more accurate normalization in the energy region below 300 keV (see [29] for the detailed description). The new normalization gives a  $S(0)=3.44 \pm 0.39$  MeV b, with an  $S(E)$  factor shown in Fig.1 as red solid dots from [23, 29] and black solid dots from [22]. Direct data are shown as open symbols as described in [29]. The blue and red ones refer to direct data of [53, 54]. The solid line represents the polynomial fit to the THM bare nucleus  $S(E)$  factor as reported in [29]. Fitting the low-energy data below  $E_{cm}=70$  keV with the screening function (Eq.2) and leaving  $U_e$  as free parameter, this provides  $U_e=350 \pm 100$  eV. The new reaction rate deviates from 5% to 15% with respect to the value reported in the NACRE compilation [52] as the temperature decreases from 1 down to  $10^{-3}$  T9 (see [29] for details). Astrophysical implications of these results have been investigated performing calculations on PMS models for  ${}^6\text{Li}$  and on the solar

**Table 1.** Two-body reactions studied via the THM with measured two-to-three body TH reactions and relevant references for each process

Direct reaction	TH reaction	ref
${}^7\text{Li}(p,\alpha){}^4\text{He}$	${}^7\text{Li}(d,\alpha\alpha)n$	[19]
${}^7\text{Li}(p,\alpha){}^4\text{He}$	${}^7\text{Li}({}^3\text{He},\alpha\alpha){}^2\text{H}$	[20]
${}^6\text{Li}(d,\alpha){}^4\text{He}$	${}^6\text{Li}({}^6\text{Li},\alpha\alpha){}^4\text{He}$	[21]
${}^6\text{Li}(p,\alpha){}^3\text{He}$	${}^6\text{Li}(d,\alpha){}^3\text{He}n$	[22, 23]
${}^{11}\text{B}(p,\alpha){}^8\text{Be}$	${}^{11}\text{B}(d,\alpha){}^8\text{Be}n$	[30]
${}^{10}\text{B}(p,\alpha){}^7\text{Be}$	${}^{10}\text{B}(d,\alpha){}^7\text{Be}n$	[31, 32]
${}^9\text{Be}(p,\alpha){}^6\text{Li}$	${}^9\text{Be}(d,\alpha){}^6\text{Li}n$	[33, 34]
${}^2\text{H}({}^3\text{He},p){}^4\text{He}$	${}^6\text{Li}({}^3\text{He},p\alpha){}^4\text{He}$	[35]
${}^2\text{H}(d,p){}^3\text{H}$	${}^2\text{H}({}^6\text{Li},t p){}^4\text{He}$	[36]
${}^{15}\text{N}(p,\alpha){}^{12}\text{C}$	${}^{15}\text{N}(p,\alpha){}^{12}\text{C}n$	[37]
${}^{18}\text{O}(p,\alpha){}^{15}\text{N}$	${}^{18}\text{O}(p,\alpha){}^{15}\text{N}n$	[38, 39]
${}^1\text{H}(p,p){}^1\text{H}$	${}^2\text{H}(p,pp)n$	[12, 13]
${}^2\text{H}(d,p){}^3\text{H}$	${}^2\text{H}({}^3\text{He},t p){}^1\text{H}$	[40, 41, 42]
${}^2\text{H}(d,n){}^3\text{He}$	${}^2\text{H}({}^3\text{He},{}^3\text{He}n){}^1\text{H}$	[40, 41, 42]
${}^{19}\text{F}(p,\alpha){}^{16}\text{O}$	${}^2\text{H}({}^{19}\text{F},\alpha){}^{16}\text{O}n$	[43]
${}^{17}\text{O}(p,\alpha){}^{14}\text{N}$	${}^2\text{H}({}^{17}\text{O},\alpha){}^{14}\text{N}n$	[44]
${}^4\text{He}({}^{12}\text{C},{}^{12}\text{C}){}^4\text{He}$	${}^6\text{Li}({}^{12}\text{C},\alpha){}^{12}\text{C}{}^2\text{H}$	[45]
$n({}^6\text{Li},t){}^4\text{He}$	${}^2\text{H}({}^6\text{Li},t){}^4\text{He}{}^1\text{H}$	[11, 46]
${}^{11}\text{B}(p,\alpha){}^8\text{Be}$	${}^2\text{H}({}^{11}\text{B},\alpha){}^8\text{Be}n$	[48]
${}^{13}\text{C}(\alpha,n){}^{16}\text{O}$	${}^6\text{Li}({}^{13}\text{C},n){}^{16}\text{O}{}^2\text{H}$	[49]

”Lithium problem” for  ${}^7\text{Li}$ . A full account is reported in [29] and [25] respectively. In particular for the  ${}^7\text{Li}(p,\alpha){}^3\text{He}$  case, it appears that the THM cross section does not significantly change the surface Lithium abundance for the present Sun, with respect to previous results reported in the NACRE compilation [52] because of the small discrepancy between the two rates. The Lithium problem for the Sun is not solved and the observed Lithium surface abundance is not reproduced by the model.

However, uncertainties on these nuclear reaction rate are now so small to move the ”Lithium problem” to astrophysics. Other input parameters such as original metallicity, helium abundance, convection efficiency and stellar mass have much larger uncertainties that seriously affect any comparison between theory and observations and need to be better constrained. Recently, the new direct data by [53, 54] have been used for a better normalization also in the  ${}^7\text{Li}(p,\alpha){}^4\text{He}$  channel [27]. The new normalization of the THM  $S(E)$  factor is shown in Fig.2 as black solid dots. Red and blue open circles represent data from [53] and [54] respectively. The other open symbols refer to direct data of [57]. The solid line represents the polynomial fit to the THM bare nucleus  $S(E)$  factor as reported in [27]. The new  $S(0)$  turns out to be  $S(0)=53 \pm 5$  keV b, while the fit of the low energy region including the screening function (Eq.2) returns a  $U_e$  value of  $U_e=425\pm 60$ eV. The updated  $S(0)$  value deviates by 4% when compared with the previous normalization in [19], while  $U_e$  deviates by about 23%. The new reaction rate experiences a variation with respect to the NACRE one [52] from about 13% at

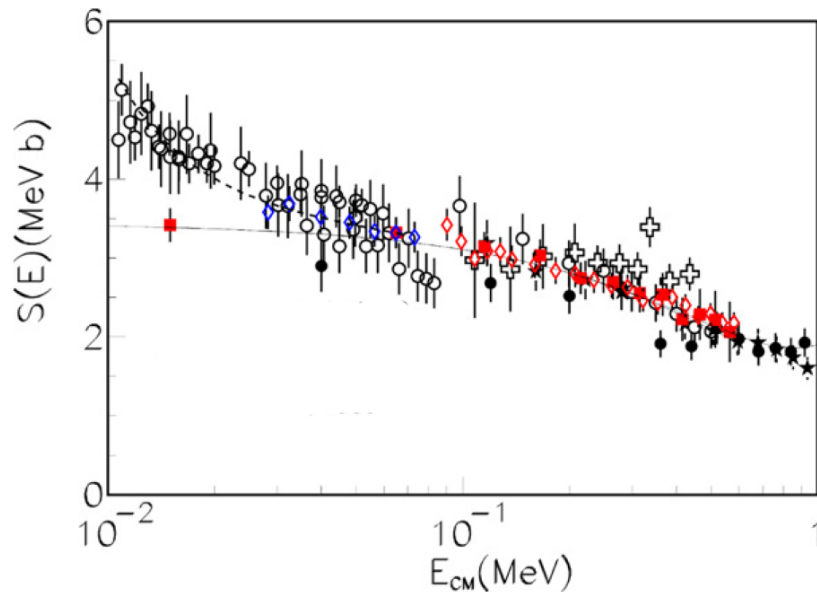


**Figure 1.** THM bare nucleus  $S(E)$  factor for the  ${}^6\text{Li}(p,\alpha){}^3\text{He}$  reaction (green solid dots from [29] and black solid dots for [22]). Direct data represented with open symbols as described in [29]. The blue and green ones refer to the most recent direct experiment reported in [53, 54]. The solid line represents the polynomial fit to the THM bare nucleus  $S(E)$  factor as reported in [29].

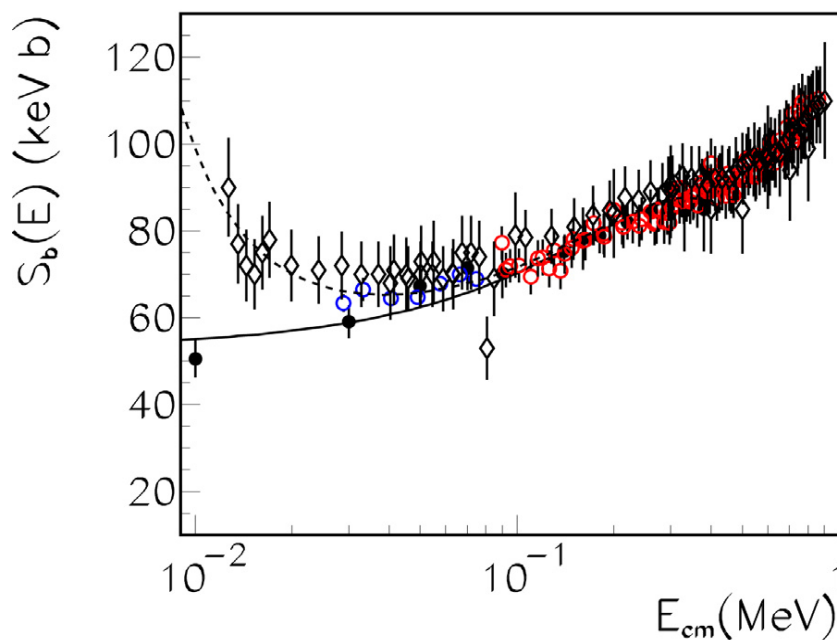


**Figure 2.** THM bare nucleus  $S(E)$  factor for the  ${}^7\text{Li}(p,\alpha){}^4\text{He}$  reaction (black solid dots from [19]). Direct data represented with open symbols as described in [27]. The red and blue open circles refer to the most recent direct experiment reported in [53] and [54] respectively. The solid line represents the polynomial fit to the THM bare nucleus  $S(E)$  factor as reported in [27].

around  $T9=10^{-3}$  to about 5% at higher temperatures and astrophysical calculations need to be readdressed for several scenarios.

## 5. Bibliography

- [1] Assenbaum HJ *et al* 1987 *Z. Phys. A* **327** 461
- [2] Strieder F *et al* 2001 *Naturwissenschaften* **88** 461
- [3] Fiorentini G *et al* 1995 *Z. Phys. A* **350** 289
- [4] Tumino A *et al* 2013 *Few Body Syst.* **54**, Issue 7-10 869
- [5] Spitaleri C *et al* 2011 *Phys. At. Nucl.* **74** 1763
- [6] Tumino A *et al* 2013 *Few Body Syst.*, **54**, Issue 5-6 745
- [7] Tumino A *et al* 2014 *Acta Physica Polonica B* **45** 181
- [8] Baur G 1986 *Phys. Lett. B* **178** 135
- [9] Kasagi J *et al* 1975 *Nucl. Phys. A* **239** 233
- [10] Mukhamedzhanov A M *et al.*, *Eur. Phys. J. A* **27** (2006) 205
- [11] Tumino A *et al* 2005 *Eur. Phys. J. A* **25** 649
- [12] Tumino A *et al* 2007 *Phys. Rev. Lett.* **98** 252502
- [13] Tumino A *et al* 2008 *Phys. Rev. C* **78** 064001
- [14] Jackson J D and Blatt J M 1950 *Rev. Mod. Phys.* **22** 77
- [15] Shapiro I S *et al* 1965 *Nucl. Phys. A* **61** 353
- [16] Jain M *et al* 1970 *Nucl. Phys. A* **153** 49
- [17] Copi C J, Schramm D N, Turner M S 1995 *Science* **627** 192
- [18] Spitaleri C *et al* 1999 *Phys. Rev. C* **60** 055802
- [19] Lattuada M *et al* 2001 *Astrophysical Journal* **562** 1076
- [20] Tumino A *et al* 2006 *Eur. Phys. J. A* direct 1 DOI: 10.1140/epja/i2006-08-038-1
- [21] Spitaleri C *et al* 2001 *Phys. Rev. C* **63** 005801
- [22] Tumino A *et al* 2003 *Phys. Rev. C* **67** 065803
- [23] Tumino A *et al* 2004 *Prog. Theor. Phys. Suppl.* **154** 341
- [24] Aliotta M *et al* 2000 *Eur. Phys. J. A* **9** 435
- [25] Pizzone RG *et al.*, *A&A* **398**, (2003) 423
- [26] Pizzone RG *et al.*, *Phys. Rev. C* **83**, (2011) 045801
- [27] Lamia L *et al* 2012 *A&A* **A185** 541
- [28] Pizzone RG *et al.* 2005 *A&A* **438** 779
- [29] Lamia L *et al* 2013 *Astrophysical J.* **768** 65
- [30] Spitaleri C *et al* 2004 *Phys. Rev. C* **63** 055806
- [31] Lamia L *et al* 2007 *Nucl. Phys. A* **787** 309
- [32] Lamia L *et al* 2008 *Il Nuovo Cimento* **31** N.4 423
- [33] Qun-Gang Wen *et al* 2008 *Phys. Rev. C* **78** 035805
- [34] Qun-Gang Wen *et al.* 2011 *J.Phys. G: Nucl. Part. Phys.*, **38** 085103
- [35] La Cognata M *et al* 2006 *Eur. Phys. J. A* **27** 249
- [36] Rinollo A *et al* 2005 *Nucl. Phys. A* **758** 146
- [37] La Cognata M *et al* 2007 *Phys. Rev. C* **76** 065804
- [38] La Cognata M *et al* 2008 *Phys. Rev. Lett.* **101** 52501
- [39] La Cognata M *et al* 2010 *Astrophysical J.* **708** 796
- [40] Tumino A *et al* 2011 *Phys. Lett. B* **700** 111
- [41] Tumino A *et al* 2011 *Phys. Lett. B* **705** 546
- [42] Tumino A *et al* 2014 *Astrophysical Journ.* **785** 96
- [43] La Cognata M *et al* 2011 *Astrophysical J. Lett.* **739** L54
- [44] Sergi ML *et al* 2010 *Phys. Rev. C* **R82** 032801
- [45] Spitaleri C *et al* 2000 *Eur. Phys. Journ.* **A7** 181
- [46] Gulino M *et al* 2010 *J.Phys. G: Nucl. Part. Phys.* **37** 125105
- [47] Lamia L *et al* 2009 *Il Nuovo Cimento*, **31** 423
- [48] Lamia L *et al* 2012 *Journ. of Phys. G: Nucl. Part. Phys.* **39** 015106
- [49] La Cognata M *et al* 2013 *Phys. Rev. Lett.* **49** 015106
- [50] Lamia L *et al* 2012 *Phys. Rev. C* **85** 025805
- [51] Grevesse N & Sauval AJ 1998, *Space Sci. Rev.*, **85** 161
- [52] Angulo C *et al* 1999 *Nucl. Phys. A* **656** 3
- [53] Cruz J *et al* 2005 *Phys. Lett. B* **624** 181
- [54] Cruz J *et al.* 2008 *Journ. of Phys. G: Nucl. Part. Phys.* **635** 192
- [55] Degl’Innocenti S *et al* 2008 *Ap&SS* **316** 25
- [56] Ciaccio F, Degl’Innocenti S & Ricci B 1997 *A&A* **123** 449
- [57] Engstler S *et al* 1992 *Z. Phys. A* **342** 471